



Investigation of Thermal and Strength Properties of a Novel Composite Developed for Insulation as Building Material

Fatih Koçyiğit¹

Received: 9 December 2019 / Accepted: 7 February 2020 / Published online: 20 February 2020
© Springer Science+Business Media, LLC, part of Springer Nature 2020

Abstract

The aim of the present study is to produce novel developed composite materials which provide thermal insulation by using waste and natural materials in construction applications. Composite construction samples were prepared using an expanded perlite aggregate of 15 % wt., 30 % wt., and 45 % wt., which had the grain sizes of 0–3 mm, 3–5 mm and 5–8 mm, as well as waste marble dust of 5 % and 15 % filtrated from a 300 μm sieve, combined with molten tragacanth of 0 %, 0.5 % and 1 %, and CEMI 42.5 N-type portland cement. The microstructure of the composite samples was examined by the SEM analysis. Density, thermal conductivity, compressive strength, abrasion loss, water absorption, compressive strength after high temperature, and compressive strength after freeze–thaw tests were performed on these composite samples. It was found that the density values of composite materials decreased from 1.983 $\text{g}\cdot\text{cm}^{-3}$ to 0.933 $\text{g}\cdot\text{cm}^{-3}$. It was observed that their porosity ratios up to 43 % were improved by increasing the amount of waste marble dust, expanded perlite and molten tragacanth, additionally, while their compressive strengths decreased. Thermal conductivity of the porous samples decreased from 0.468 $\text{W}\cdot\text{m}^{-1}\cdot\text{K}^{-1}$ to 0.167 $\text{W}\cdot\text{m}^{-1}\cdot\text{K}^{-1}$ by raising their porosity, which corresponds to a reduction of 36%. It was observed that as the rates and sizes of the materials used in the samples, their thermal conductivity, compressive strength and density values decreased, and the abrasion loss and water absorption increased.

Keywords Building material conductivity · Insulation · Insulation composite · Thermal and strength properties of composite · Thermal conductivity

Symbols and Abbreviations

AL	Abrasion loss (%)
avr	Average
c	Cement
d	Dry

✉ Fatih Koçyiğit
fatih.kocyyigit@dicle.edu.tr

¹ School of Civil Aviation, Dicle University, Diyarbakır, Turkey

ep	Expanded perlite
Md	Marble dust
t	Tragacanth
w	Wet
WA	Water absorption (%)
ρ	Density ($\text{g}\cdot\text{cm}^{-3}$)
Φ	Porosity (%)
1	Startup
2	Finish

1 Introduction

The amount of consumption of energy resources required for heating buildings has gradually increased in a wasteful way, due to the number of buildings increasing in parallel with the population growth worldwide, and this negatively affects the ecosystem of our planet in terms of environmental pollution [1]. Regarding shelter and heating, which are basic needs of human beings, the construction of buildings which are resistant to earthquakes and consume less energy, comes into prominence.

For earthquake-resistant buildings, low density, namely lightweight concretes must be used [2]. The usage and investigation of lightweight concretes are increasing day by day due to their low density, low thermal conductivity value, and architectural flexibility properties. Lightweight concretes with superior properties, such as thermal and sound insulation, have significant advantages compared to normal concretes due to energy savings and comfort. These studies have mainly focused on the addition of different aggregates into the cement [3]. One of the materials used as an aggregate in production of lightweight concrete is expanded perlite. Thermal conductivity of expanded perlite is $0.040\text{--}0.06 \text{ W}\cdot\text{m}^{-1}\cdot\text{K}^{-1}$ [4]. Through expanded perlite, it is important to keep the internal temperatures of indoor spaces in the structures at the desired level, to save energy using expanded perlite in the heating and cooling processes of external climatic conditions, to solve environmental problems, to reduce air pollution, and most importantly, to take thermal insulation measures [5]. Due to its high thermal, sound insulation qualities and low-cost properties, the market share of expanded perlite in the construction sector in Turkey has quadrupled in the last decade [6]. As a result of using the blocks of expanded perlite in structures, 35 % to 45 % heat saving is achieved compared to conventional construction materials. The thermal insulation property of the expanded perlite block is closely related to the block geometry, which is a function of the expanded perlite aggregate forming the block and the properties of the mixture [7]. The strength of lightweight concrete with expanded perlite can be increased somewhat by taking some measures during its production [8]. International studies have been conducted on many natural aggregates (such as diatomite, pumice, slag, shavings, palm oil shells and bottom ash) or artificial aggregates (such as expanded clay, slag, slate, perlite and vermiculite) for the production of mortar or concrete [9–15]. Finding new and improved ways to build structures with natural volcanic materials (such as perlite and ash) is becoming increasingly common, and their use as construction materials can lead to

low-cost structures. It is important to evaluate marble waste, having technological and economic values, together with expanded perlite in the production of composite construction elements in terms of adaptation to the environment and recycling strategies. Dust wastes obtained as production waste in marble plants cannot be generally utilized, and their storage or disposal to a natural environment can cause environmental pollution and problems, such as the pollutions of natural resources [16]. In the studies conducted on the assessment of the materials discarded to waste sites in marble processing plants, the dust wastes were reduced to different size fractions, except for their use as construction material, they are used in many fields [17]. Soykan and Özel [18] investigated the use of marble waste as an aggregate in polymer concrete technology. Aruntaş et al. [19] investigated the physical, chemical and mechanical properties of the samples, obtained by mixing waste marble dust doped with Portland cement in various dosages, at different curing times. Türker et al. [20] examined the effects of waste marble dusts on the hydration levels and microstructure of cement. Şengül et al. [21] replaced expanded perlite with a natural aggregate in lightweight concrete mixtures and investigated the effect of their thermal insulation properties. Demirboğa and Gül [22] examined the compressive strength and thermal conductivity of concretes containing mineral-doped expanded perlite aggregate. Öztürk [23] aimed to produce a thermal-insulated lightweight concrete using lightweight aggregate (pumice, perlite, EPS) in the concrete and determined the 7–28-day mechanical and physical properties of the produced lightweight concrete. Demirboğa and Gül [24] investigated the effects of expanded perlite aggregate, silica fume, and fly ash on the thermal conductivity of lightweight concrete.

Tragacanth used in the study is a kind of viscous, odorless, tasteless, and water-soluble gum obtained by drying resin, naturally exuding or exuded from the trunk of a thorn named as *Astragalus* from Leguminosae family, under natural conditions. The gum exudes from the plant as bended strips or cut flakes. It absorbs water to be a gel that can become a paste [25]. Since the thermal conductivity of the molten tragacanth is $0.155 \text{ W}\cdot\text{m}^{-1}\cdot\text{K}^{-1}$ [26], its use in composite mixtures reduces its thermal conductivity further. Differently from the literature, this study aimed to produce a new construction material using the molten tragacanth, which is a natural resin, together with waste marble dust and expanded perlite aggregate and to investigate its thermal and strength properties.

2 Materials and Methods

2.1 Materials

To prepare the samples, the crude perlite was supplied from the perlite deposits in İzmir Bergama Region and it was broken and expanded at $800 \text{ }^\circ\text{C}$ in a furnace. As seen in Fig. 1, the samples were divided in three groups based on 0–3 mm, 3–5 mm, and 5–8 mm grain sizes. The waste marble dust was used by drying the slurry wastes, coming out during the production of marbles produced by Dimer Diyarbakır Mermer ve Maden İşletmesi San. ve Tic. A.Ş., in the oven and milling them in a $300 \text{ }\mu\text{m}$ sieve. Gum tragacanth was powderized with the help of an



Fig. 1 Expanded perlite aggregates sized as 0–3 mm, 3–5 mm, 5–8 mm

electric motor grinder. 100 g of powdered tragacanth was weighed using a Tem NS 6200 device with a sensitivity of 0.1 g and put in a 5 L water container, then 2 L of water was added and mixed thoroughly. The mixing process was continued at certain intervals for 1 day. After the tragacanth was thoroughly disintegrated and swelled, 1 L of water was added into the mixture at 1–2 h intervals, and the mixing process continued. After tragacanth–water mixture became 5 L, the mixture was filtrated 2 times and transferred to another vessel. The aim of the filtering process is to clean the non-melting particles, such as sand or herbal residue, in the tragacanth and to transform the melt into a homogeneous mixture [26]. It was determined that 100 gr tragacanth homogeneously dissolved in 5 L of water. Once the powdered tragacanth became a homogeneous melt together with water, it was involved as a fluid mixture in the study.

Expanded perlite aggregate of 15 wt%, 30 wt%, and 45 wt%, which had the grain sizes of 0–3 mm, 3–5 mm and 5–8 mm, as well as waste marble dust of 5 % and 15 % filtrated from a 300 μm sieve, molten tragacanth of 0 %, 0.5 % and 1 %, and cement were used to prepare the samples. While forming the mixture, first the necessary rate of expanded perlite and waste marble dust was weighed using a precision balance and then transferred to the mixture bucket. The same process was also performed for the cement and the necessary rate of cement was added into the vessel for that series of samples. The three materials were mixed by using a trowel. Finally, a mixture of molten tragacanth at the calculated rate was added to the mixture. The mixtures were stirred for approximately 3 min. The mixtures were put in 20 mm \times 60 mm \times 150 mm plywood molds to determine their thermal conductivity and water absorption values. On the other hand, some of the mixture was put in 100 mm \times 100 mm \times 100 mm molds to determine the compressive strength, abrasion loss, compressive strength after high temperature and compressive strength after a freeze–thaw process.

The samples were kept in the mold for 24 h and then taken out and allowed to set for 28 days at room temperature. They were placed into the oven set to 105 ± 5 $^{\circ}\text{C}$, and they were dried until the weight was found to be constant. Figure 2 shows the experimental flowchart for production process of construction

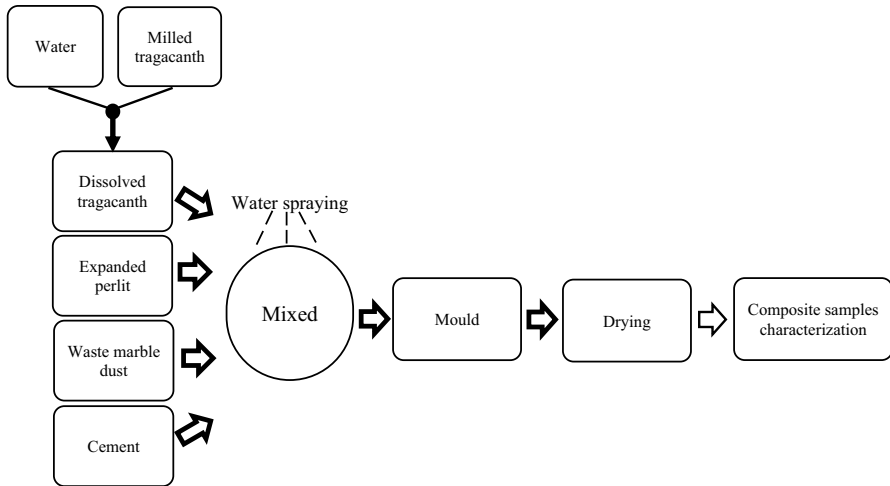


Fig. 2 Experimental flowchart for building materials process



Fig. 3 Laminated (a) and molten (b) appearance of the tragacanth

materials. Figure 3 shows the gum form of the tragacanth used in the tests and its appearance after being dissolving in water.

Table 1 shows the physical and chemical properties of the expanded perlite aggregate used in experimentals. Table 2 shows the physical and chemical properties of the waste marble dust used in experimentals. Table 3 shows the chemical properties of the tragacanth used in experimentals.

2.2 Thermal Conductivity Tests

We performed the thermal conductivity tests in the Bartın University, the Mechanical Engineering Faculty Construction Department's Laboratories (Bartın, Turkey). A Shotherm Quick Thermal Conductivity Meter (QTM) based on DIN 51046 hot wire method was used (ASTM C 1113-90) in measuring thermal conductivity [29]. The

Table 1 Chemical and physical properties of the expanded perlite [27]

Components	Weight percentage (%)
SiO ₂	72.3
Al ₂ O ₃	13.4
Na ₂ O	3.15
K ₂ O	4.81
CaO	0.83
Fe ₂ O ₃	0.51
MgO	0.12
TiO ₂	0.09
Grain sizes (mm)	Specific weight (kg m ⁻³)
0–3	267
3–5	252
5–8	215

Table 2 Physical and chemical properties of marble dust [28]

Specific weight (g·cm ⁻³)	2.71
Specific surface (cm ² g ⁻¹)	4372
SiO ₂ (%)	0.94
Fe ₂ O ₃ (%)	0.46
Al ₂ O ₃ (%)	15.20
CaCO ₃ (%)	34.20
MgO (%)	0.65

major advantage of this method is to be able to measure the actual thermal conductivity without changing the humidity level of the material even if the material heterogeneous [26]. In the measurement method of the Shotherm QTM-D2 device, the probe is placed on the material to be measured. Measuring time is 100–120 s as the standard.

The measurement range of the device is 0.02–10 W·m⁻¹·K⁻¹. The device measures the thermal conductivity of the samples with an uncertainty of 5 % [30]. The Shotherm QTM-D2 device was calibrated by a polymer of 0.241 W·m⁻¹·K⁻¹ thermal conductivity, provided for this purpose by the manufacturer. To determine thermal conductivity of the samples produced each sample was measured three times and once their arithmetic means were taken, their thermal conductivity was determined.

2.3 Mechanical Tests

We performed the mechanical tests in the Dicle University, Engineering Faculty Mining Engineering Construction Department's laboratories (Diyarbakır,

Table 3 Chemical, thermal and conductivity analysis properties of tragacanth (these results are obtained according to the Dumas Method)

Elementary analysis	C: 65.77 %; N: 0.25 %; S: 11.78 %; H: – %; O: – %
Thermal analysis	The structure is stable up to 116 °C (No mass loss) 94.5 % of the structure was decomposed between 226 °C and 327 °C and caused mass loss.
Conductivity	284 $\mu\text{S cm}^{-1}$ (27 °C)

Turkey). The compressive strength, abrasion loss (AL), water absorption (WA), and density were evaluated for each sample using test procedures described in the TS 699 (2009) standard [31].

The compressive strength and abrasion loss tests were applied to the 100 mm × 100 mm × 100 mm samples. The compressive strength tests applied on the samples were performed using an Elle International brand device that has 3000 kN loading capacity, a digital command panel, and an adjustable loading rate and can apply force at single axis. It was preferred to measure the weight reduction to find abrasion loss in the samples via friction and this process was performed via the “Bohme” device. The abrasion loss (AL) values were calculated using Eq. 1 [26].

$$\%AL = \frac{\text{Firstmass} - \text{Lastmass}}{\text{Firstmass}} \times 100 \quad (1)$$

In the water absorption test, the test samples with the sizes of 20 mm × 60 mm × 150 mm were placed into the oven adjusted to 105 ± 5 °C, and they were dried until the weight was found to be constant. In this way, the powders on the samples which weight was made constant were weighed at a sensitivity of 0.1 g after they were cleaned using a brush and the dry sample weights (W_d) were determined. These samples were placed in a vessel containing water at a depth corresponding to 1/4 of the sample height at room temperature. Water was added into the vessel in such a way for 1/2 of the height of the sample to be under water 1 h later and for 3/4 of its height to be under water 2 h later. 24 h after the tests, water was added into the vessel so that the samples were completely under the water [26].

After the samples were kept for 24 h, they were removed from the water, wiped with a piece of cloth, immediately weighed by a precision balance and their water-absorbed weights were found (W_w). By taking the ratio of these two weights, the percentage of water absorption was calculated as “%” in the following Eq. 2.

$$WA\% = \frac{W_w - W_d}{W_d} \times 100 \quad (2)$$

The density measurement of the samples with the sizes of 20 mm × 60 mm × 150 mm was performed using the Isomet 2104 heat transfer analyzer of Applied Precision Company. The device has been developed especially to determine the thermo-physical properties of construction elements, natural stone and soil.

The SEM analysis was performed on 100 mm × 100 mm × 100 mm samples and the tests of compressive strength after high temperature and compressive strength after freeze–thaw were applied. We performed the SEM analysis by the JEOL JSM 7001F scanning microscope within the body of the FUEM laboratory of Fırat University (Elazığ, Turkey). In this process, an electron current of 0.25 mm diameter was transferred on the sample with the help of magnetic lenses (electron guns). The samples were moved in horizontal and vertical axes and the desired structures or phases were examined in detail. The desired point of the sample examined could be analyzed [32]. During the SEM analysis conducted to examine the internal structure of the samples, a detailed topographical study was performed on the surfaces of the

samples by applying 10–20 kV accelerated electron bombardment on the samples in an electron microscope.

The high-temperature application was realized by applying the temperatures of 400 °C, 600 °C, and 800 °C to the samples in the Protherm HLF 150 laboratory type oven with the capacity of 1200 °C and the heating rate of 6 °C·min⁻¹ for 1 h. The oven operating at target temperatures for 1 h automatically turned off and the samples were left to cool until room temperature with approximately 2 °C·min⁻¹ cooling rate in the oven. Compressive strength was applied to all the samples after a high temperature test.

The freeze–thaw test was performed by freezing the samples at -20 ± 2 °C in accordance with ASTM C 666-92 and thawing them in 20 ± 2 °C of water at room temperature [33]. The samples prepared were made waterlogged and placed in the freezer. After they were kept in the freezer at -20 °C, they were left to dissolve at $+20$ °C. The freeze–thaw process was accepted as 1 cycle and 30 cycles were applied to all samples. After this freeze–thaw process was repeated, the samples were dried in the oven until they reached to a constant mass at 110 ± 5 °C and then they were cooled until room temperature and they were subject to the compressive strength test.

3 Results and Discussion

Density is one of the important parameters that can control the amount of construction materials and many physical properties in the production of lightweight concretes. It was observed that the porosity increased and accordingly the thermal conductivity decreased due to the decreased density. Table 4 shows the measurement results of density, porosity, thermal conductivity, compressive strength, abrasion loss, and water absorption ratio.

In the samples in which the expanded perlite grain size, expanded perlite ratio, and molten tragacanth ratio were the same but the rate of waste marble dust increased; the thermal conductivity and the compressive strength decreased since the waste marble dust could not fill the gaps in the sample and the amount of cement decreased [19]. The high pore amount of the sample and the low thermal conductivity of the gasses in the pore led to low thermal conductivity of the samples produced. However, when composite samples were exposed to a humid environment, the gasses in the pores are replaced with water or water vapor; therefore, the thermal conductivity of the composite increases depending on the rate of water with a thermal conductivity approximately 20 times greater [24]. Such changes may vary based on the density change of the sample. Figure 4 shows the change in the thermal conductivity depending on the mixture rates of the samples. Table 4 shows the density, thermal conductivity, compressive strength, abrasion loss rate, and the water absorption rate of the composite samples. All samples were according to the ratio of tragacanth, the particle diameters of expanded perlite and waste marble dust were coded with numbers. These codes are explained in Table 4.

In the above plots, the amount of molten tragacanth and waste marble dust in expanded perlite samples having the same sizes and rates decreased with the thermal

Table 4 Measurement results of the produced composite samples

Sample code	Density (g·cm ⁻³)	Porosity (%)	Thermal conductivity (k (W·m ⁻¹ ·K ⁻¹))	Compressive strength (MPa)	Abrasion loss (%)	Water absorption (%)
Samples with 0.0 % tragacanth ratio						
X110	1.983	0.264	0.468	33.25	0.68	19.56
X210	1.878	0.285	0.437	29.21	0.86	20.75
X310	1.762	0.308	0.394	26.30	1.06	21.18
X120	1.662	0.320	0.381	30.39	0.79	20.55
X220	1.645	0.337	0.359	27.31	0.97	20.84
X320	1.593	0.370	0.334	25.63	1.17	22.32
Y110	1.744	0.356	0.447	31.08	0.78	21.20
Y210	1.692	0.412	0.419	27.22	0.99	22.03
Y310	1.645	0.428	0.359	25.31	1.21	22.50
Y120	1.593	0.435	0.350	29.30	0.85	21.50
Y220	1.563	0.464	0.268	26.44	1.01	22.31
Y320	1.511	0.488	0.257	24.17	1.30	23.37
Z110	1.645	0.461	0.432	28.30	0.92	21.51
Z210	1.516	0.524	0.390	24.01	1.33	22.20
Z310	1.406	0.534	0.327	22.06	1.49	22.58
Z120	1.634	0.540	0.248	25.29	1.26	21.74
Z220	1.534	0.545	0.239	23.23	1.43	22.37
Z320	1.493	0.552	0.234	21.55	1.63	23.77
Samples with 0.5 % tragacanth ratio						
X111	1.779	0.272	0.379	28.09	0.91	24.39
X211	1.721	0.297	0.336	24.05	1.09	25.58
X311	1.634	0.314	0.286	21.14	1.29	26.01

Table 4 (continued)

Sample code	Density ($\text{g}\cdot\text{cm}^{-3}$)	Porosity (%)	Thermal conductivity (k) ($\text{W}\cdot\text{m}^{-1}\cdot\text{K}^{-1}$)	Compressive strength (MPa)	Abrasion loss (%)	Water absorption (%)
X121	1.616	0.327	0.275	25.22	1.02	25.38
X221	1.529	0.345	0.267	22.14	1.20	25.67
X321	1.464	0.386	0.237	20.46	1.40	27.15
Y111	1.628	0.365	0.345	25.91	1.01	26.03
Y211	1.552	0.424	0.311	22.05	1.22	26.86
Y311	1.516	0.436	0.268	20.14	1.44	27.33
Y121	1.476	0.442	0.260	24.13	1.08	26.33
Y221	1.447	0.473	0.219	21.27	1.24	27.14
Y321	1.347	0.501	0.213	19.01	1.53	28.20
Z111	1.301	0.470	0.336	23.13	1.16	26.34
Z211	1.266	0.529	0.299	18.85	1.56	27.03
Z311	1.219	0.539	0.249	16.89	1.72	27.41
Z121	1.155	0.543	0.212	20.13	1.49	26.57
Z221	1.132	0.548	0.207	18.06	1.66	27.20
Z321	1.079	0.559	0.202	16.38	1.86	28.60
Samples with 1 % tragacanth ratio						
X112	1.634	0.276	0.349	24.80	1.10	30.35
X212	1.575	0.309	0.305	21.81	1.28	31.53
X312	1.488	0.318	0.290	18.90	1.48	31.96
X122	1.470	0.333	0.263	22.98	1.21	31.33
X222	1.383	0.355	0.224	19.91	1.39	31.63
X322	1.319	0.398	0.213	18.23	1.59	33.11
Y112	1.482	0.371	0.328	23.68	1.20	31.98

Table 4 (continued)

Sample code	Density (g·cm ⁻³)	Porosity (%)	Thermal conductivity (k) (W·m ⁻¹ ·K ⁻¹)	Compressive strength (MPa)	Abrasion loss (%)	Water absorption (%)
Y212	1.406	0.438	0.296	19.81	1.41	32.81
Y312	1.371	0.444	0.257	17.90	1.63	33.29
Y122	1.330	0.450	0.217	21.89	1.27	32.29
Y222	1.301	0.484	0.201	19.04	1.43	33.10
Y322	1.201	0.512	0.191	16.77	1.72	34.16
Z112	1.155	0.480	0.319	20.90	1.34	32.30
Z212	1.120	0.537	0.277	16.61	1.75	32.98
Z312	1.073	0.547	0.232	14.66	1.91	33.36
Z122	0.986	0.553	0.188	17.89	1.68	32.52
Z222	0.971	0.565	0.175	15.82	1.85	33.15
Z322	0.933	0.608	0.167	14.14	2.05	34.56
<i>The first number (diameter)</i>						
X:	Expanded perlite (0–3 mm)					
Y:	Expanded perlite (3–5 mm)					
Z:	Expanded perlite (5–8 mm)					
<i>The second number (ratio)</i>						
1:	Expanded perlite (15 %)					
2:	Expanded perlite (30 %)					
3:	Expanded perlite (45 %)					
<i>The third number (ratio)</i>						
1:	Waste marble dust (5 %)					
2:	Waste marble dust (15 %)					
<i>The fourth number (ratio)</i>						
0:	Tragacanth (0.0 %)					
1:	Tragacanth (0.5 %)					
2:	Tragacanth (1 %)					

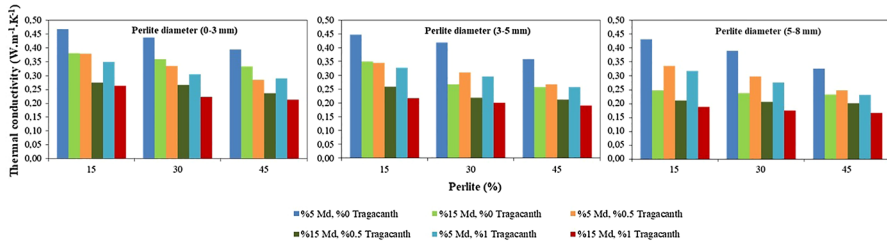


Fig. 4 The change in thermal conductivity depending on the ratios of expanded perlite, waste marble dust and molten tragacanth

conductivity. One of the most important reasons for this was that the molten tragacanth had a low thermal conductivity, sticks to the entire surface and transfers its effect to other materials and the waste marble dust led to a crystalized structure in the sample [18]. As this crystalized structure did not exhibit adhesion in the sample, it created pore and reduced thermal conductivity. Another reason was that the liquid tragacanth carried its air-filled pores into the mixture at the end of the drying and formed artificial pores.

In the present study, the lowest thermal conductivity ($0.167 \text{ W}\cdot\text{m}^{-1}\cdot\text{K}^{-1}$) belonged to the sample no. Z322 containing the expanded perlite with the grain size of 5–8 mm at 45 wt%, waste marble dust at 15 wt%, and the molten tragacanth at 1 wt%. The highest thermal conductivity of $0.468 \text{ W}\cdot\text{m}^{-1}\cdot\text{K}^{-1}$ belonged to the sample no. X120 containing the expanded perlite with the grain size of 0–3 mm at 15 wt%, waste marble dust at 5 wt%, and without molten tragacanth. At the end of measurement, the thermal conductivity of the waste marble dust was $0.690 \text{ W}\cdot\text{m}^{-1}\cdot\text{K}^{-1}$, the thermal conductivity of the molten tragacanth was $0.155 \text{ W}\cdot\text{m}^{-1}\cdot\text{K}^{-1}$, and the thermal conductivity of the cement was $0.450 \text{ W}\cdot\text{m}^{-1}\cdot\text{K}^{-1}$. It was observed that the thermal conductivity of the waste marble dust and cement were high and their strength values varied according to their mixture rates.

When examining the compressive strength of the samples in Table 4, it was observed that compressive strength of the samples with the grain size of 0–3 mm varied in the range of 18.23 and 33.25 MPa. Compressive strength of those with the grain size of 3–5 mm varied in the range of 16.77 and 31.08 MPa, and compressive strength of the samples with the grain size of 5–8 mm varied in the range of 14.14 and 28.30 MPa.

Figure 5 shows the effects of sizes and rates of the materials in the sample for each of three types on compressive strength. Depending on the increase of the molten tragacanth used in the sample, compressive strength decreased. Additionally, it was observed that the waste marble dust increased the pore ratio in the sample and decreased the strength values. Another reason was that the compressive strength of the samples decreased with the increase of the grain size of the expanded perlite.

The results in Table 4 show that the samples containing expanded perlite with large grain size and higher ratios of waste marble dust and molten tragacanth among the mixtures used in the tests were not abrasion resistant. It was observed that the abrasion resistance decreased with the increase in the ratio of waste marble dust.

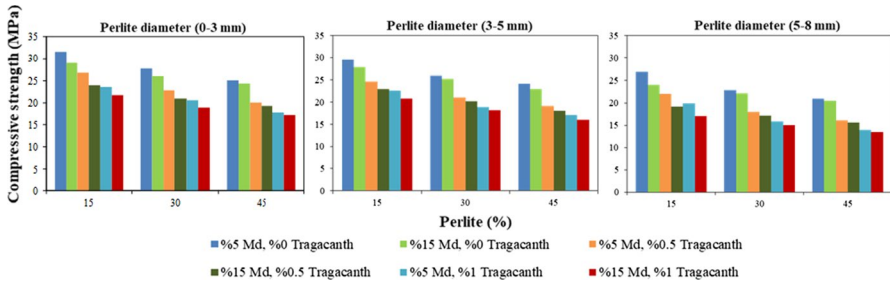


Fig. 5 The change in the compressive strength depending on the ratios of expanded perlite, waste marble dust and molten tragacanth

Figure 6 shows the effect of expanded perlite, waste marble dust, and molten tragacanth on friction and abrasion loss. It was determined that the samples with expanded perlite grain sizes of 0–3 mm, 3–5 mm, and 5–8 mm as well as the samples with a molten tragacanth rate of 1 %, expanded perlite rate of 45 % and waste marble dust rate of 15 % were not abrasion resistant.

The abrasion loss rate of the samples produced with expanded perlite aggregates with the grain size of 0–3 mm varied between 0.68 and 1.59. The abrasion loss of the samples produced with expanded perlite aggregates with the grain size of 3–5 mm varied between 0.78 and 1.72. The abrasion loss of the samples produced with expanded perlite aggregates with the grain size of 5–8 mm varied between 0.92 and 2.05. As seen from the results of water absorption tests in Table 4, it was determined that the water absorption rate of some of the samples was higher than 30 %, which is the critical value in the literature. The samples had a hollow structure, and the porosity ratio varied within the whole structure based on the grain size of the expanded perlite, the rate of expanded perlite and the rate of the waste marble dust. This increased the water absorption capacity and the water absorption values of the samples by allowing them to retain water in these gaps when the samples were contacted with water. Figure 7 shows water absorption ratio of the samples.

As seen from Fig. 7, the water absorption rate of the samples with the grain size of 0–3 mm varied between 19.56 % and 33.11 %, the water absorption rate of the samples with the grain size of 3–5 mm varied between 21.20 % and 34.16 %, and

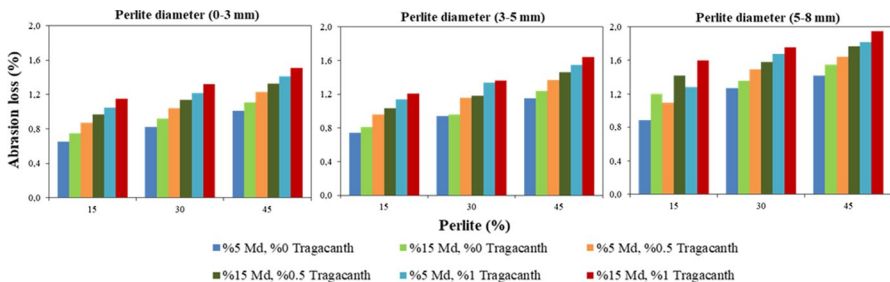


Fig. 6 The change in the abrasion loss depending on the ratios of expanded perlite, waste marble dust, and molten tragacanth

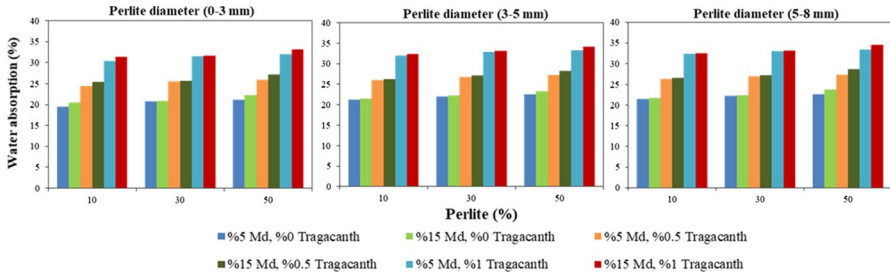


Fig. 7 The change in the water absorption ratio, depending on the ratios of expanded perlite, waste marble dust, and molten tragacanth

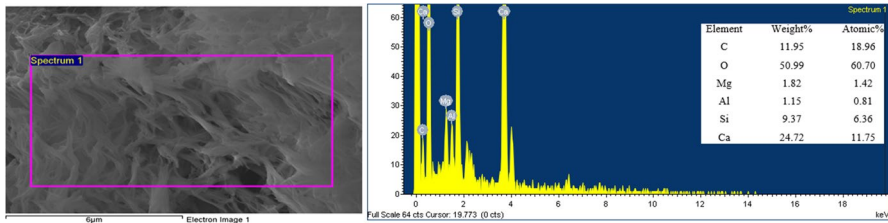


Fig. 8 Pore and cracks formed by the molten tragacanth in the sample and spectrum curve of the elements within the sample

water absorption rate of the samples with the grain size of 5–8 mm varied between 21.51 % and 34.56 %. SEM (Scanning Electron Microscope) analyses was carried out to examine the internal structures of the samples obtained within the scope of the present study. During the SEM analysis, a detailed topographical study was performed about the surface of the sample no. Z322 in the electron microscope by applying 10–20 kV accelerated electron bombardment.

It was observed that the porosity in the sample increased due to the density rate of molten tragacanth in the spectrum curve of the elements in sample no. Z322 in Fig. 8 and in the SEM images of the sample no. Z322 in Fig. 9. Adhesion was achieved in the sample with the dense melt tragacanth, resulting in increased gaps due to perlite and waste marble dust. This caused a decrease in the strength properties of the samples and improvements in their thermal conductivity properties.

The experimental results indicated that compressive strength could be preserved at the temperatures varying between 20 °C and 400 °C. Significant losses in compressive strength occur between 400 °C and 600 °C. Most of the compressive strength is lost between 600 °C and 800 °C [34–36]. The plots in Fig. 10 shows that the strength decreased due to the effect of high temperature. While the highest compressive strength value belonged to the X110 series without tragacanth, 5 % waste marble dust, and 15 % expanded perlite with the grain size of 0–3 mm at 400 °C, the lowest compressive strength value belonged to the Z322 series containing 45 % expanded perlite with the grain size of 5–8 mm at 800 °C, 1 % tragacanth, and 15 % waste marble dust. Considerable decreases were observed such as 25.95

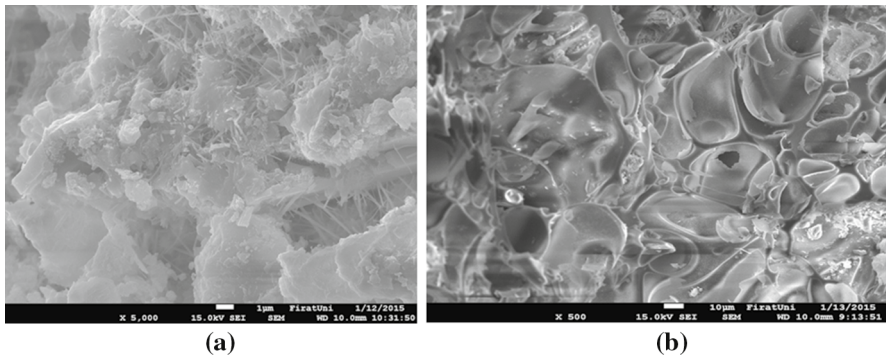


Fig. 9 Distribution of the molten tragacanth in the sample

% in compressive strength values of the samples after 400 °C compared to the control samples, 44.20 % in compressive strength values of the samples after 600 °C compared to the control samples, and 67.20 % in compressive strength values of the samples after 800 °C compared to the control samples.

Figure 11 shows the plot showing the change in the compressive strength of the samples after a freeze–thaw process. The plots show that the values of compressive strength after a freeze–thaw process decreased since the other materials in the sample and waste marble dust were not sufficiently adhered to each other as a result of the increase of waste marble dust. The decrease of the gaps in the structure of the sample also increased the compressive strength after a freeze–thaw process. The increases in the grain size of the expanded perlite, the rate of the expanded perlite, the molten tragacanth rate and the rate of the waste marble dust decreased the compressive strength of the samples. The compressive strengths after the freeze–thaw process in the samples decreased by 5.06 % and 11.84 % compared to the control samples.

4 Conclusions

In the study, density, thermal conductivity, water absorption, compressive strength, abrasion loss, compressive strength after high temperature, and compressive strength after freeze–thaw experiments were performed, respectively, on the composite samples prepared and the following results were obtained.

- The molten tragacanth being used as a liquid mixture instead of distilled water decreased its thermal conductivity by providing adherence within the composite sample and forming extra artificial pores.
- The increase of sizes and rates of the materials in the samples increased the pore ratio and insulation properties and led to lower thermal conductivity. With increasing pore ratio, densities of the materials decreased. This indicated that there was a direct proportion between density and thermal conductivity.

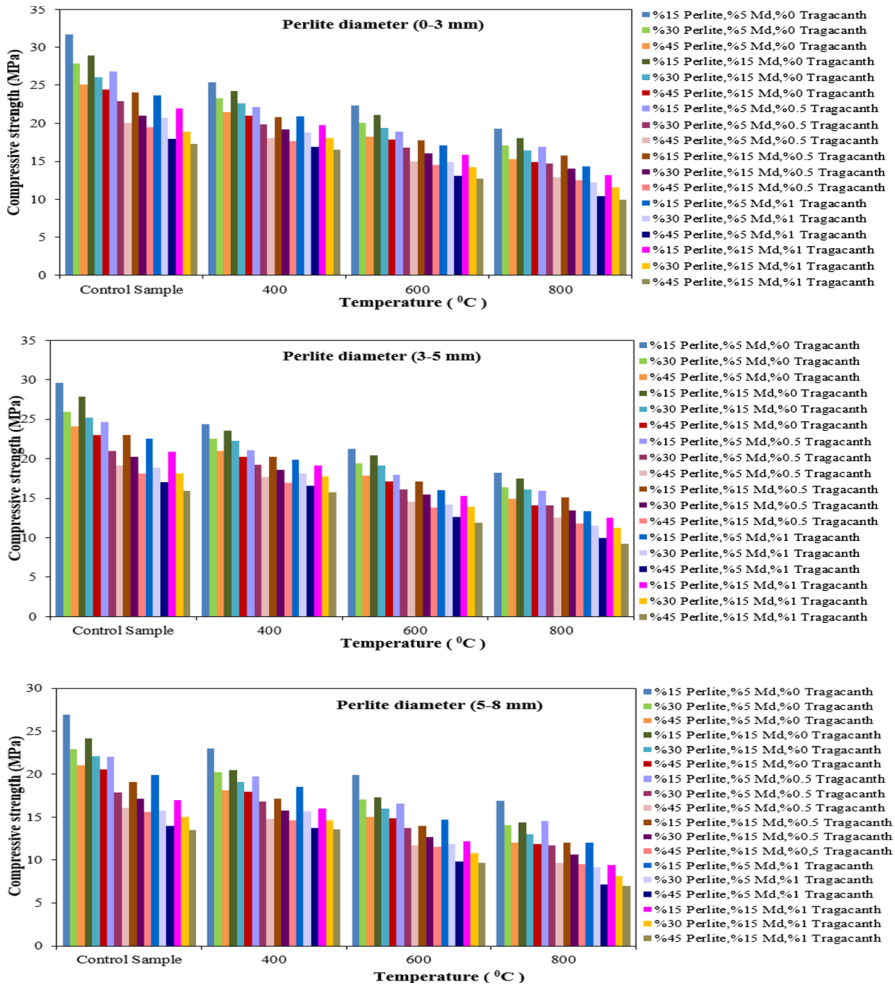


Fig. 10 The change in the compressive strength of the samples after high temperature

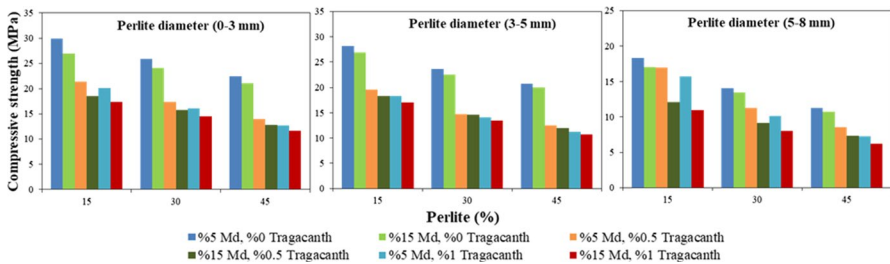


Fig. 11 The change in the compressive strength of the samples after freezing and thawing

- The lowest thermal conductivity among the composite samples prepared was $0.167 \text{ W}\cdot\text{m}^{-1}\cdot\text{K}^{-1}$ and obtained from the sample no. Z322.
- The pore ratios in the sample varied depending on the rate of waste marble dust. Since waste marble dust did not provide adherence in the sample, thermal conductivity and compressive strength decreased and abrasion loss and water absorption rates increased with increasing the rate of waste marble dust.
- Tragacanth provided adhesion within the samples and increased the WA (water absorption) ratios by creating an extra artificial pore. The reason for the increase in water absorption rate was that water got easily diffused through capillary channels in the pores.
- Major compressive strength losses occurred between $400 \text{ }^\circ\text{C}$ and $600 \text{ }^\circ\text{C}$ in high temperature tests and after the freeze–thaw process.
- The highest AL (abrasion loss) rate was observed in the samples with high waste marble dust and molten tragacanth rates.

Consequently, when it is desired to save energy by thermal insulation in the constructions, it is possible to prefer the sample no. Z322, having lowest thermal conductivity in the study. Since strength of the sample no. Z322 is low, it can be used as an intermediate filling material on the sandwich walls or as a roof insulation material in the structures, as well as building applications such as panels, cladding walls, composite floor systems, internal partitions, and insulating plaster on the interior walls. For the production of lightweight construction materials, expanded perlite, waste marble dust and molten tragacanth can be used as alternative raw material resources. It should be noted that this type of lightweight concrete produced is weaker under load compared to normal concrete. They should not be used at the places directly exposed to water. Covering the surface of the samples with waterproofing materials may prevent the capillary absorption of water and lead to additional costs.

Compliance with Ethical Standards

Conflict of interest The author declares no conflict of interests.

References

1. M. Záleská, M. Pavlikova, J. Pokorný, O. Jankovský, Z. Pavlík, R. Černý, *Constr. Build. Mater.* **180**, 1 (2018)
2. C. Tasdemir, O. Sengul, M.A. Tasdemir, *Energy Build.* **151**, 469 (2017)
3. M. Lanzón, P.A. García-Ruiz, *Constr. Build. Mater.* **22**, 1798 (2008)
4. H. Shoukry, M.F. Kotkata, S.A. Abo-EL-Enein, M.S. Morsy, S.S. Shebl, *Constr. Build. Mater.* **102**, 167 (2016)
5. H. Doğan, F. Şener, *News Bull.* **1**, 51 (2004)
6. Y. E. Çiçek, Comparative examination of physical, chemical, and mechanical properties of terracotta, brick, pumice concrete, gas concrete and perlite construction materials, Phd. thesis. (ITU Institute of Science, Istanbul, 2002)
7. ETİ Holding Corp., Perlit Mine Directorate. *Istanbul Bull.* **67**, 37–38 (2003)

8. S. Azizi, Mechanical Properties and thermal insulation of perlite-doped lightweight concretes, PhD thesis, (ITU Institute of Science, Istanbul, 2015)
9. K. Ayse, K.A.R. Filiz, *Constr. Build. Mater.* **105**, 572 (2016)
10. M.J. Shannag, *Constr. Build. Mater.* **25**, 658 (2011)
11. K.M.A. Hossain, M. Lachemi, *ACI Mater. J.* **103**, 11 (2006)
12. K.M.A. Hossain, S. Ahmed, M. Lachemi, *Constr. Build. Mater.* **25**, 1186 (2011)
13. H.A. Gavligi, Tragacanth gum: structural composition, natural functionality and enzymatic conversion as source of potential prebiotic activity, PhD thesis, (Technical University of Denmark, Lyngby, 2012)
14. F. Koksall, O. Gencel, W. Brostow, H.H. Lobland, *Mater. Res. Innov.* **16**, 7 (2012)
15. R.T. Hemmings, B.J. Cornelius, P. Yuran, Comparative study of lightweight aggregates. in *Proceedings of the World of Coal Ash*, (Lexington, 2009)
16. M. Sutcu, H. Alptekin, E. Erdogmus, Y. Er, O. Gencel, *Constr. Build. Mater.* **82**, 1 (2015)
17. E.T. Tunc, *J. Environ. Manag.* **231**, 86 (2019)
18. O. Soykan, C. Özel, The effect of marble dust grain size on properties of polymer concrete, (International Construction Congress, October 11-13, Isparta, 2012)
19. H.Y. Aruntaş, M. Gürü, M. Dayı, I. Tekin, *Mater. Des.* **31**, 4039 (2010)
20. P. Türker, B. Erdoğan, F. Katnaş, A. Yağınobalı, Classification and properties of fly ashes in Turkey, (Publications of Turkish Cement Manufacturers' Association, 2003), pp. 76–77
21. O. Sengül, S. Azizi, F. Karaosmanoglu, M.A. Tasdemir, *Energy Build.* **43**, 671 (2011)
22. R. Demirboğa, R. Gül, *Energy Build.* **35**, 1155 (2003)
23. D. Shastri, H.S. Kim, *Constr. Build. Mater.* **60**, 1 (2014)
24. R. Demirboğa, R. Gül, *Cem. Concr. Res.* **33**, 723 (2003)
25. Y. Bicer, S. Yılmaz, *Eng. Technol.* **7**, 24 (2013)
26. F. Kocyigit, Evaluation of pumice and cement mixture with tragacanth as a new building material, PhD Thesis, (Firat University, Elazığ, 2012)
27. Bergama Mining Perlite Factory Trade Corporation, <http://www.bergamaperlite.com/>. Accessed 21 Nov 2019
28. Dimer Marble and Mine Factory Trade Corporation, <http://www.dimer.com.tr/>. Accessed 15 Oct 2019
29. ASTM C1113/C1113M-09, Test method for thermal conductivity of refractories by hot wire (Platinum Resistance Thermometer Technique, 2013)
30. E.K. Akpınar, F. Koçyigit, *J. Adhes. Sci. Technol.* **30**, 534 (2016)
31. J. Wyrwal, A. Marynowicz, J. Swirska, *Bauphysik* **30**, 431 (2008)
32. T. Kavas, Production of refractory cement by using waste marble and aluminum hydroxide, PhD Thesis (Osmangazi University Institute of Science, Eskisehir, 2003)
33. ASTM C 666-92, Standard test method for resistance of concrete to rapid freezing and thawing, vol. 04.02 (Concrete and Aggregates, American Society for Testing and Materials, 1999)
34. Z. Huang, J.R. Liew, W. Li, *Constr. Build. Mater.* **148**, 579 (2017)
35. X. Luo, W. Sun, S.Y.N. Chan, *Cem. Concr. Res.* **30**, 379 (2000)
36. M.B. Karakoç, *Constr. Build. Mater.* **41**, 21 (2013)

Publisher's Note Springer Nature remains neutral with regard to jurisdictional claims in published maps and institutional affiliations.